ELSEVIER

PII: S0032-3861(96)00970-6

Polymer Vol. 38 No. 15, pp. 3921–3925, 1997

0032-3861/97/$17.00 + 0.00

Polymer–polymer interface in polypropylene/polyamide blends by reactive processing

Hongguo Li, Tsuneo Chiba, Noboru Higashida, Ying Yang and Takashi Inoue*

Department of Organic and Polymeric Materials, Tokyo Institute of Technology, Ookayama, Meguro-ku, Tokyo 152, Japan
(Received 17 August 1996)

Reactive blending of polypropylene (PP) and amorphous polyamide (aPA) was carried out using a gram-scale mixer. Maleic anhydride-grafted PP was used as a reactive PP. Time-resolved light scattering analysis showed that, compared with non-reactive systems, the reactive one yielded finer particles of sub-μm, via a faster size-reduction process, and exhibited better stability of dispersed particles for static annealing, suggesting the emulsifying effect of *in situ* formed PP–aPA graft copolymer. Both ellipsometry and transmission electron microscopy showed that the interface established in the reactive system was very thick ($\sim$ 40 nm); it was several times the coil size of the component polymer. The thick interface is assumed to be a layer of accumulated micelles of the *in situ* formed graft copolymer. In the thick interface, instead of cross-hatched lamellar crystallites, long lamellar crystals were found to develop. © 1997 Elsevier Science Ltd.

(Keywords: polypropylene; polyamide; blend; reactive processing; interface; graft copolymer)

INTRODUCTION

Much attention is being paid to the reactive processing of immiscible polymers. This approach is effective in the control of morphology and in the design of high-performance polymer blends, such as rubber-toughened plastics and thermoplastic elastomers. Reactive processing involves *in situ* reaction of functionalized components to form a block or graft copolymer at the interface between the phases[1–10]. The copolymer is believed to play the role of an emulsifier, which provides a fine morphology and increases the adhesive strength between the two phases. However, so far there have been limited studies on the interface of blends prepared by reactive processing.

In this paper, we deal with polypropylene (PP)/polyamide (PA) systems. The PP/PA is the first and memorable combination on which the reactive processing was undertaken by Ide and Hasegawa[1]. They employed maleic anhydride-grafted PP (PP–MAH) and demonstrated the reaction between MAH sites on PP and the amino-chain end of PA to form a PP/PA graft copolymer. Recently, the relationship between morphology and mechanical properties of the reactive PP/PA system was studied by several groups[11,12]. To obtain a deeper understanding of the polymer–polymer interface in this reactive system, we carried out a melt blending using a miniature mixer, investigated the size reduction of dispersed particles during processing and the stability of particle dispersion during static annealing by light scattering, and analysed the interface by ellipsometry and transmission electron microscopy (TEM).

* To whom correspondence should be addressed

EXPERIMENTAL

The PP used in this study was a commercial isotactic PP (J3HG, Mitsui-Toatsu Co.; $M_w = 50 \times 10^3$). PP–MAH was provided by Sumitomo Chemical Industry ($M_w = 60 \times 10^3$, MAH content = 0.08 wt%). As PA specimen, we used an amorphous nylon, (aPA) (Grilamide TR55LX®, EMS Japan Co.; $M_w = 50 \times 10^3$, $T_g = 97°C$). It is reported that the aPA was prepared by polycondensation of isophthalic acid, 4,4′-diamino-3,3′-dimethyldicyclohexylmethane and laurolactone. We chose this PA, since we were able to carry out mixing experiments and interfacial analysis at relatively low temperatures, at which there is less problem of thermal degradation as compared with the cases of PA6 and PA66, which have high melting points.

Melt mixing was carried out in a miniature mixer, Mini-Max Molder (CS-183 MM, Custom Scientific Instruments) at 240°C with a rotor speed set at 100 rev min^{-1}. The weight ratio of (PP + PP–MAH)/PA was fixed at 70/30. The PP–MAH content was varied from 0 to 100 wt%. During the mixing, a small amount of mixed melt was extruded at appropriate intervals. The extruded melt was quickly quenched in liquid nitrogen to freeze the two-phase structure in the melt. Thus, we prepared a series of mixed-and-quenched specimens with various residence times in the mixer. The specimens were subjected to light scattering and TEM analyses as follows.

The quenched specimen was placed between two cover

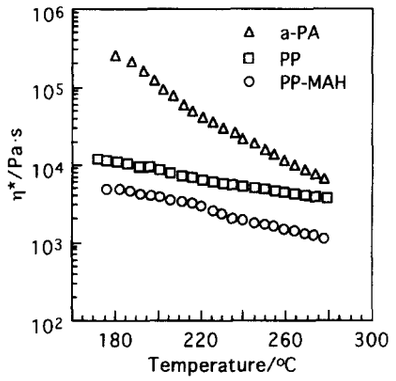

Figure 1 Temperature dependence of the melt viscosity of component polymers: the dynamic complex viscosity at $\omega = 10\,\text{rad}\,\text{s}^{-1}$

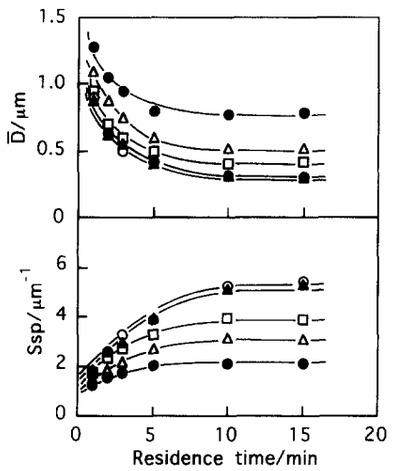

Figure 2 Time variation of (a) average particle size $\bar{D}$, and (b) specific interfacial area S_{sp}, during melt mixing at 240°C. Composition in (PP + PPN − MAH)/aPA: ●, (70 + 0)/30; △, (69 + 1)/30; □, (65 + 5)/30; ○, (35 + 35)/30; ▲, (0 + 70)/30

glasses and melt-pressed to a thin film (~ 20 μm thick) at 240°C on a hot stage set on a light scattering apparatus. Immediately after the melt-pressing, the time-resolved measurement of scattering profile (angular dependence of scattered light intensity) with a time slice of 1/30 s was started. The scattering apparatus consisted of a 46 photodiode array, a He–Ne laser of 632.8 nm wavelength and V_v (parallel polarization) optical alignment [9]. Since the two-phase structure in the melt is in a non-equilibrium state, it coarsens with time after the re-melt. A scattering profile just after the re-melt provides information on the two-phase structure in the mixed-and-quenched mixture. By the time variation of scattering profile, one can discuss the structure coarsening during isothermal annealing, which may be affected by the *in situ* formed PP–PA graft copolymer.

The quenched specimen was first stained by a 10% aqueous solution of phosphotungstic acid at room temperature for four days, then by RuO_4 gas at 50°C for 2 h. The stained specimen was cut into ultra-thin sections of 70 nm thickness at −60°C by an ultramicrotome, Ultracut S (Leica Co.). TEM observation was carried out by a transmission electron microscope (Hitachi EM H-300), applying an acceleration voltage of 75 kV.

The quenched specimen was fractured in liquid nitrogen and the fractured surface was observed by scanning electron microscopy (SEM), JSM-T220 (Jeol Co.).

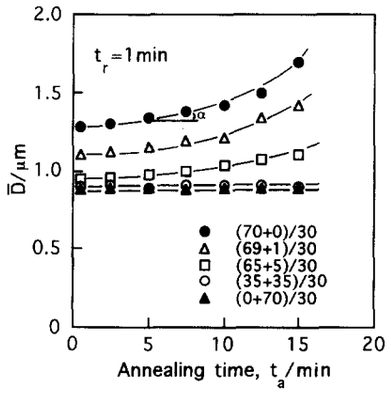

Figure 3 Time variation of average particle size $\bar{D}$ during static annealing at 240°C after melt mixing for 1 min. Slope α may be the coalescence rate (symbols are the same as in *Figure 2*)

To estimate the interfacial thickness by ellipsometry, we prepared a bilayer specimen consisting of a thin (*ca* 200 nm) PP (or PP–MAH) film and a thick (*ca* 0.5 mm) PA substrate. The substrate was prepared by melt-pressing between two silicon wafers to create an optically flat surface. The thin film was prepared by spin-coating of a 4 wt% solution in xylene on to a silicon wafer. The latter was mounted on the former by floating-on-water and pick-up technique[13,14]. The bilayer specimen thus prepared was dried under vacuum (10^{-2} Pa) at 50°C for 24 h. Ellipsometric analysis was carried out by an automated ellipsometer[15] and the interfacial thickness was measured as a function of time of annealing at high temperatures (200–240°C). Details of the apparatus and the analysis can be found elsewhere[14,15].

RESULTS AND DISCUSSION

The dynamic complex viscosity η^* is plotted as a function of temperature for the component polymers in *Figure 1*.

All specimens in this study exhibited a light scattering profile of a monotonical decreasing function, i.e. the intensity of scattering light, I, decreased monotonically with increasing scattering angle, θ. From such scattering profiles, one can obtain a series of morphology parameters by the Debye–Bueche plot, i.e. by the plot of $I(q)^{-1/2}$ *versus* q^2, where q is the magnitude of the scattering vector, given by $q = (4\pi/\lambda')\sin(\theta/2)$, λ' being the wavelength of light in the specimen[16]. When the plots are observed to be linear, the correlation distance ξ is given by the slope and intercept of the $I(q)^{-1/2}$ axis by

$$I(q)^{-1/2} = (8\pi\langle\eta^2\rangle\xi^3)^{-1/2}(1 + \xi^2 q^2) \quad (1)$$

where $\langle\eta^2\rangle$ is the mean-square fluctuation of the refractive index. Once the value of ξ is given, other morphology parameters such as the specific interfacial area S_{sp} and the mean diameter of dispersed particles $\bar{D}$ are obtained by

$$S_{sp} = 4\phi(1 - \phi)\xi^{-1} \quad (2)$$

$$\bar{D} = 6\phi S_{sp}^{-1} \quad (3)$$

where ϕ is the volume fraction of the dispersed phase.

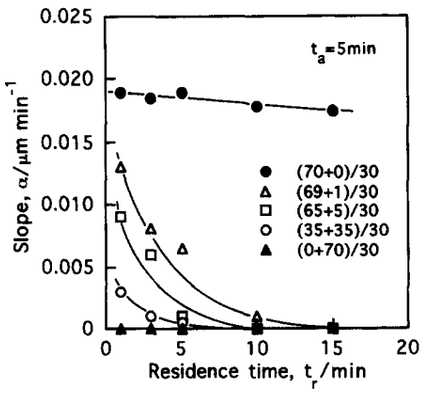

Figure 4 Coalescence rate α *versus* residence time in mixer t_r (symbols are the same as in *Figures 2* and *3*)

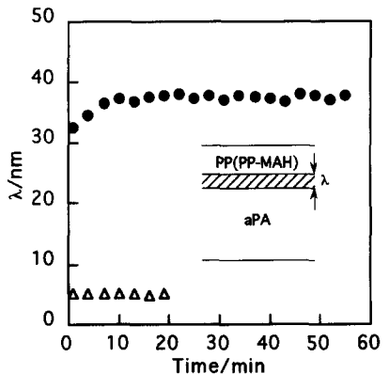

Figure 5 Interfacial thickness λ *versus* annealing time at 200°C: ●, reactive system (PP–MAH/aPA); △, non-reactive system (PP/aPA)

The morphology parameters thus obtained are plotted as a function of residence time t_r in *Figure 2*. One sees the systematic size reduction and interface evolution during melt mixing and the effect of reactive component (PP–MAH) on them. PP–MAH has a lower melt viscosity than PP (see *Figure 1*). When the amount of PP–MAH is increased, the melt viscosity of the matrix is expected to decrease. The reduction of matrix viscosity is expected to provide a negative effect on the size reduction of dispersed particles. In contrast, a positive effect is seen in *Figure 2*. The positive effect may be caused by the *in situ* formation of PP/aPA graft copolymer at interface.

In *Figure 3* are shown the time variations of $\bar{D}$ during static annealing at 240°C. All specimens here are after melt mixing for 1 min ($t_r = 1$ min). One sees that in the non-reactive system (●; PP–MAH = 0 phr), $\bar{D}$ increases with annealing time t_a. It suggests that coalescence takes place during the annealing. In contrast, $\bar{D}$ of the reactive system containing a large amount of PP–MAH (○, 35 phr; ▲, 70 phr) remains constant, suggesting that the graft copolymers prevent the coalescence. Note that such a morphology stabilization mechanism is already set up in a short residence (reaction) time ($t_r = 1$ min).

As a measure of coalescence rate, one may employ a slope of $\bar{D}$ *versus* t_a plot in *Figure 3*. The slope α is plotted as a function of residence time in *Figure 4*. One can see that, even in a low PP–MAH content system (○, 1 phr), a good stabilization mechanism is established after residence for 10 min ($t_r = 10$ min), suggesting sufficient coverage of the interface by the *in situ* formed graft copolymers, which provide the entropic repulsion

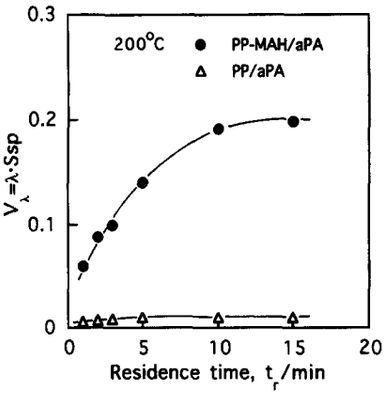

Figure 6 Interface evolution in terms of the increase in volume fraction of interface V_λ with time of mixing

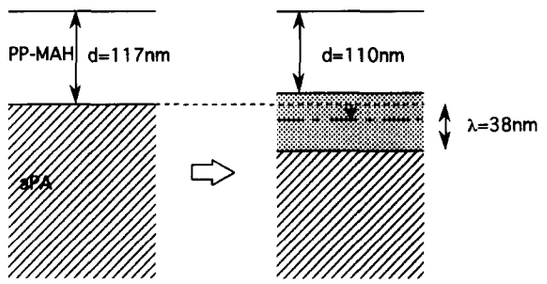

Figure 7 Schematic representation of asymmetric interface development in a reactive system

between neighbouring particles. The higher the PP–MAH content, the shorter the t_r the mechanism is set up in.

The results of ellipsometric analysis on interfacial thickness are shown in *Figure 5*. Compared with the non-reactive system, the reactive system attained a very thick interface ($\lambda \sim 40$ nm). It is much larger than the coil size of the component polymers: the root-mean-square radius of gyration $\langle s^2 \rangle^{1/2} = 3.7 \times 10^{-2} M_w^{1/2} \sim 10$ nm for PP[17].

Such extremely thick interfaces have also been observed in other systems: an aPA/styrenic copolymer containing poly(styrene-*co*-maleic anhydride)[15] and poly(ethylene terephthalate)/functionalized ethylene–propylene rubber[18]. Discussion on extremely thick interfaces in reactive systems will be given later, in connection with the results of TEM observation. Combining the results of $\lambda(t)$ in *Figure 5** and $S_{sp}(t)$ in *Figure 2*, one can calculate another interfacial parameter, V_λ, the volume fraction of interface:

$$V_\lambda = \lambda \cdot S_{sp} \tag{4}$$

The results are shown in *Figure 6*. A large difference between the reactive and non-reactive systems clearly shows how effective is the reaction for the interface evolution.

In addition to the interfacial thickness, λ, the thickness d of a thin film (PP layer) can be measured by ellipsometry. The results are shown in *Figure 7*. The

* The λ values in *Figure 5* are at 200°C, while the S_{sp} values in *Figure 2* are at 240°C. The λ values at 240°C should be used for V_λ in *Figure 6*. However, at temperatures above 200°C, the bilayer specimen became wavy so that ellipsometric data were not reproducible. We then used the λ value at 200°C. Note that in the temperature range 190–220°C, λ had a very weak temperature dependence

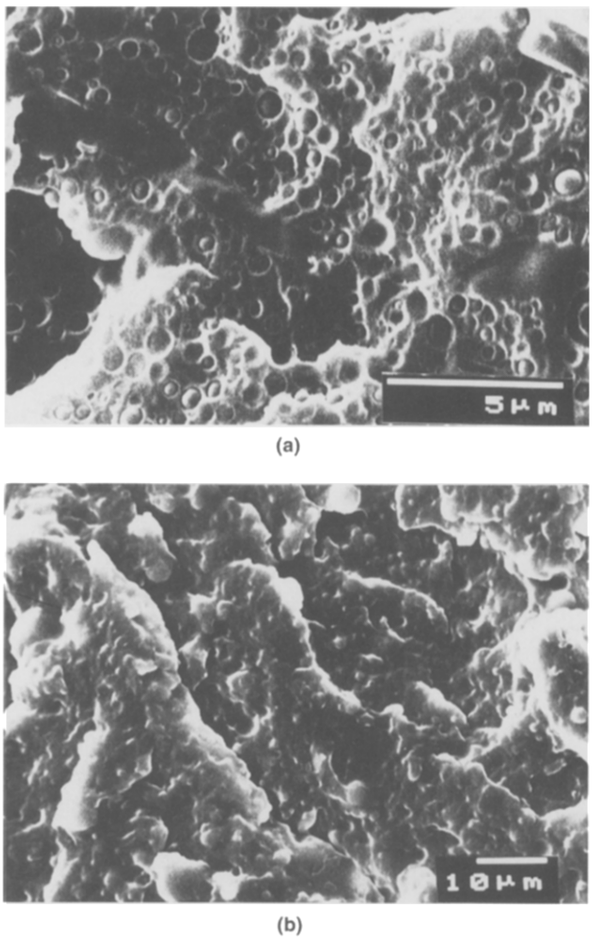

Figure 8 SEM micrographs: (a) 70/30 PP/aPA blend, and (b) 70/30 PP–MAH/aPA blend, melt-mixed at 240°C for 10 min

thickness of the PP–MAH layer hardly changes with annealing (reaction) at 200°C, while the thick interface is created. It implies that the position of (the centre) interface shifts towards the aPA side. That is, the Kirkendall effect[19] is realized at the reactive interface. It may be caused by the large difference in chain diffusivity between aPA and PP–MAH (see *Figure 1*).

Figure 8a is a SEM micrograph of a 70/30 PP/aPA blend (non-reactive system). Debonding between matrix and dispersed particles seems to take place and individual aPA particles are clearly seen. The average particle size agrees well with that by light scattering (*Figure 2*). In contrast, in the reactive system, 70/30 PP–MAH/aPA blend, it is hard to discern the individual particles (*Figure 8b*). It may suggest a strong adhesion between aPA and PP–MAH as expected from the ellipsometric result, and a complicated plastic deformation of the PP matrix thereof.

In the TEM observation of the mixed-and-quenched blend, if one pays attention to large particles with small curvature, one can obtain information on the interface which may be comparable to that of the bilayer specimen for ellipsometry. TEM images of the non-reactive (70/30 PP/aPA) and reactive (70/30 PP–MAH/aPA) systems are shown in *Figures 9a* and *9b*, respectively. In the non-reactive system, the interface is hardly discerned as a layer around aPA particles. This is expected from the result of ellipsometry, i.e. the very thin interface

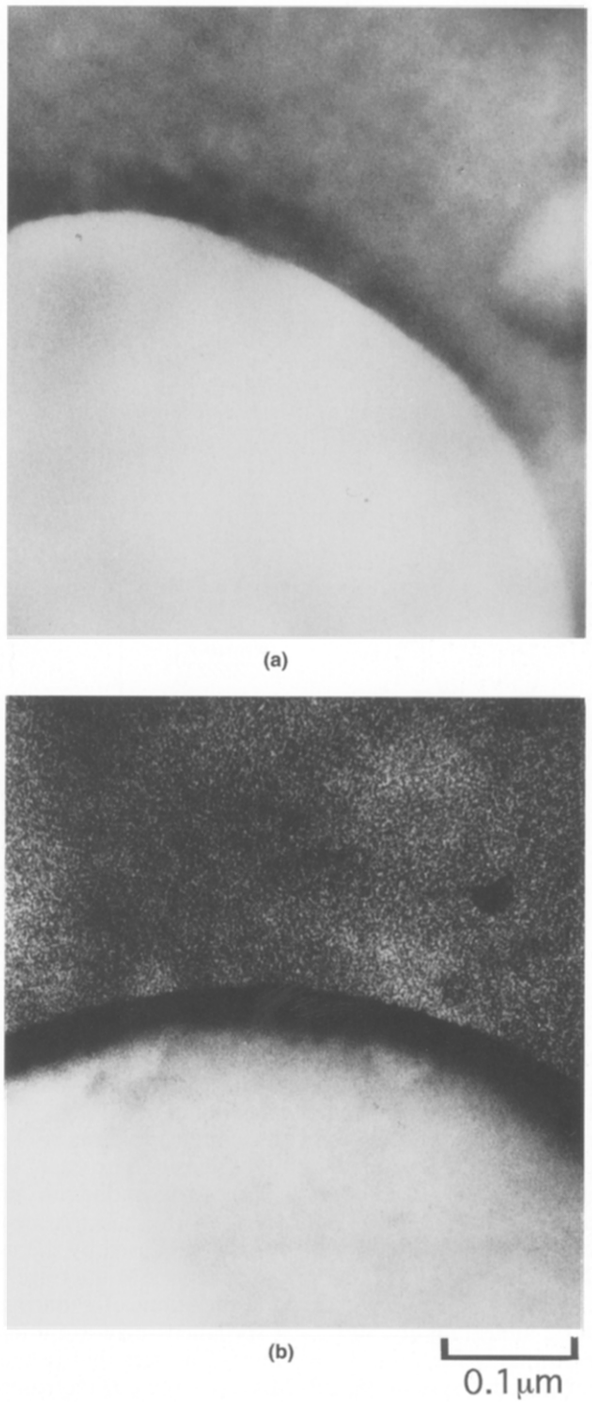

Figure 9 TEM micrographs: (a) 70/30 PP/aPA blend, and (b) 70/30 PP–MAH/aPA blend, melt-mixed at 240°C for 10 min

($\lambda = 4.8$ nm in *Figure 5*). In contrast, the reactive system definitely has a dark layer* which may be assigned to the interface. The thickness of the layer is *ca* 40 nm. It is very close to the interfacial thickness by ellipsometry shown in *Figure 5*.

Figure 10 is the TEM micrograph of the same

* It is well known that PP is stained by RuO_4[20] and PA by phosphotungstic acid[10]. In this study, we employed double staining. The double staining was accidentally found to be effective for deep staining of interface. The reason is not obvious at present

Figure 10 TEM micrograph of 7/3 PP–MAH/aPA blend, melt-mixed at 240°C for 10 min and then annealed at 140°C for 30 min

specimen as in *Figure 9b*. However, the TEM micrograph of *Figure 10* was taken after annealing at 140°C for 3 h to enhance the crystallization of PP–MAH. Again, the thick interface is clearly seen as the dark layer between the PP–MAH matrix and aPA particles. A cross-hatched crystal lamellar structure is clearly seen in the PP–MAH matrix. In the interface indicated by a white arrow, one can see long lamellae arranged in parallel with each other. The graft aPA chains may prevent the cross-hatching characteristic of the crystallization of PP. The growth of such crystal lamellae strongly supports the fact that PP–MAH chains had existed in the dark layer before the annealing (*Figure 9b*), i.e. the dark layer had consisted of PP–MAH and aPA.

Furthermore, one can see dark spots near the interface indicated by the black arrow. The spots could be assigned to the PP cores of PP–aPA graft copolymer micelles. Such micelles have been observed in reactive blends of anionically polymerized polystyrene (PS) and poly(methyl methacrylate) (PMMA) with narrow molecular weight distribution, when PS–PMMA block copolymer is formed *in situ* in excess, in much higher content than for full coverage of dispersed particles[21]. At the interface (indicated by a black arrow in *Figure 10*), where the microphase separation is achieved at a high level, the crystallization could not occur since the PP component is dispersed as the micelle core so that crystal lamellae are not seen there. When the micelles are accumulated near the interface, the accumulated layer could be observed as the thick interface by ellipsometry and TEM. This may be an interpretation for the extremely thick interface seen in *Figures 5* and *9b*.

CONCLUSION

Compared with non-reactive melt mixing, the reactive processing rendered faster size reduction, finer particle size, better morphology stability and a much thicker interface. A unique crystallization of PP was found to take place at the thick interface. The thick interface is assumed to be a layer of accumulated micelles of *in situ* formed graft copolymer.

REFERENCES

1. Ide, F. and Hasegawa, A., *J. Appl. Polym. Sci.*, 1974, **18,** 963.
2. Baker, W. E. and Saleen, M., *Polym. Eng. Sci.*, 1987, **27,** 1634.
3. Angola, J. C., Fujita, Y., Sakai, T. and Inoue, T., *J. Polym. Sci., Polym. Phys. Edn.*, 1988, **26,** 807.
4. Cecere, A., Greco, R., Ragosta, G., Scarinzi, G. and Taglialatela, A., *Polymer*, 1990, **31,** 1239.
5. Kim, B. K. and Park, S. J. *J. Appl. Polym. Sci.*, 1992, **43,** 357.
6. Teh, J. H. and Rudin, A., *Polym. Eng. Sci.*, 1992, **32,** 1678.
7. Liang, Z. and Williams, H. L., *J. Appl. Polym. Sci.*, 1992, **44,** 699.
8. Oshinski, A. J., Keskkula, H. and Paul, D. R., *Polymer*, 1992, **33,** 268.
9. Okamoto, M. and Inoue, T., *Polym. Eng. Sci.*, 1993, **33,** 175.
10. Hosoda, S., Kojima, K., Kanda, Y. and Aoyagi, M., *Polym. Net. Blend.*, 1991, **1,** 51.
11. Duvall, J., Sellitti, A., Myers, C., Hiltner, A. and Baer, E., *J. Appl. Polym. Sci.*, 1994, **52,** 195.
12. Montiel, A. G., Keskkula, H. and Paul, D. R., *Polymer*, 1995, **36,** 4587.
13. Yukioka, S. and Inoue, T., *Polym. Commun.*, 1991, **32,** 17.
14. Yukioka, S., Nagato, K. and Inoue, T., *Polymer*, 1992, **33,** 1171.
15. Yukioka, S. and Inoue, T., *Polymer*, 1994, **35,** 1182.
16. Debye, P. and Bueche, A. M., *J. Appl. Phys.*, 1949, **20,** 518.
17. Brandrup, J. and Immergut, E. H. (ed.), *Polymer Handbook.* Interscience, New York, 1967, pp. IV–48.
18. Yokoyama, K., Fujita, Y., Higashida, N. and Inoue, T., *Macromol. Symp.*, 1994, **83,** 157.
19. Wu, S., Chuang, H.-K. and Han, C. D., *J. Polym. Phys.*, 1986, **24,** 143.
20. Sano, H., Usami, T. and Nakagawa, H., *Polymer*, 1986, **27,** 1497.
21. Nakayama, A., Inoue, T., Guegan, P. and Macosko, C. W. *ACS Polym. Prepr.*, 1994, **27,** 4993.